Online appendix for "Endogenous Separations and Non-monotone Beveridge Curve Shifts"

Contents

A Solution method: details

The canonical endogenous job destruction model generates highly nonlinear unemployment dynamics, because the endogenous job-destruction cutoff moves along the cross-sectional idiosyncratic match quality distribution. We analyze the model through a lens of global nonlinear solution that is obtained from the sequence-based approach developed in Lee (2025).

One of the most challenging steps in obtaining the global solution of the dynamic stochastic general equilibrium (DSGE, hereafter) models lies in specifying the correct law of motion of the endogenous aggregate allocation: the law of motion can be correctly specified when the exact solution is known, while the solution can be obtained only after the law of motion is correctly specified. The repeated transition method overcomes this hurdle by utilizing the ergodicity of DSGE models. Under the ergodicity, if the simulated path is long enough, all the possible equilibrium allocations are realized on the simulated path. Then, the rationally expected state-contingent future outcomes can be correctly specified by combining the expected outcomes realized on the path without specifying the law of motion for these endogenous allocations.

Suppose an agent is at period t where the optimal consumption and saving decision requires specifying the rationally expected future value or marginal value. A classic state space-based approach requires the law of motion for the endogenous aggregate state, followed by the interpolation step to obtain the state-contingent value or marginal value functions. In contrast, the repeated transition method requires only identifying a period with the outcome realizations the same as each contingent state realization for period $t+1$.

Algorithm illustration We elaborate on the detailed steps for the algorithm based on our baseline model.

1. Simulate a T-period simulation path of the exogenous aggregate shock process

$\{A_t\}_{t=0}^{T}$, where T is large enough.[1]

2. For an ith iteration, guess the time series of the following allocations:[2]

$$\{n_t^{(i)}, q_t^{(i)}, v_t^{(i)}, u_t^{(i)}, c_t^{(i)}, w_t^{(i)}, \widetilde{Z}_t^{(i)}, \overline{Z}_t^{(i)}, H_t^{(i)}\}_{t=1}^{T}.$$

3. Solve the problem backward from the terminal period T, applying the repeated-transition method technique to the optimality conditions. This technique is elaborated in detail in the next section. For example, calculate the right-hand side (RHS) of the job destruction condition:

$$RHS_t^{(i)} = \beta \mathbb{E}_t \left[(1 - H_{t+1}^{(rv)}) \left(\frac{c_{t+1}^{(rv)}}{c_t^{(i)}} \right)^{-\sigma} \left(A_{t+1}^{(rv)} \overline{Z}_{t+1}^{(rv)} - w_{t+1}^{(rv)} + (1-\lambda) \frac{\kappa}{q_{t+1}^{(rv)}} \right) \right] \tag{1}$$

Then, using RHS, obtain q_t^* as follows:

$$q_t^* = \frac{\kappa}{RHS_t^{(i)}}.$$

In Equation (1), the superscript (rv) means that the allocation is a random variable. Likewise, from the backward solution, we obtain

$$\{q_t^*, v_t^*, w_t^*, c_t^*, \widetilde{Z}_t^*, \overline{Z}_t^*, H_t^*\}_{t=1}^{T}.$$

4. Using the conditionally optimal allocations with superscript $*$, we simulate allocations forward starting from period 0 to obtain the other conditionally optimal

[1] The aggregate productivity process is discretized by the Tauchen method using 11 grid points for the three-standard deviation range, and T is set at 5,000.

[2] We use the pre-computed steady-state level as the initial guess for all periods.

allocations. For example,

$$n_t^* = (1 - H_t^*)[(1 - \lambda)n_{t-1}^* + v_{t-1}^* q_{t-1}^*] \tag{2}$$

where n_0^* is fixed as the steady-state employment level.[3] Then, we obtain the following conditionally optimal allocations:

$$\{n_t^*, u_t^*\}_{t=1}^T.$$

5. Check if the following inequality is satisfied:[4]

$$tol > \sup_{y \in \Omega} \sup_t ||y_t^* - y_t^{(i)}||$$
$$where \quad \Omega = \{n, q, v, u, c, w, \widetilde{Z}, \overline{Z}, H\}$$

6. If the inequality is satisfied, ith guess is the solution. Otherwise, we update the guess using the following convex combination and return to step 3.

$$y_t^{(i+1)} = \omega y_t^{(i)} + (1 - \omega) y_t^*, \ \text{for} \forall t$$
$$\text{for } y \in \Omega = \{n, q, v, u, c, w, \widetilde{Z}, \overline{Z}, H\}.$$

ω is the weight on the previous iteration's allocation.

The convergence of the method hinges on the stability and the uniqueness of the equilibrium.

In Step 3 of the algorithm, it is necessary to identify state contingent allocations for the following variables:

$$\{H_{t+1}^{rv}, c_{t+1}^{rv}, \overline{Z}_{t+1}^{rv}, w_{t+1}^{rv}, q_{t+1}^{rv}\}$$

[3] The stability of the solution helps the path converge to the equilibrium level after several periods.
[4] tol is the tolerance level for the convergence criterion.

Due to the ergodicity of the simulated path, we can find a period where the endogenous aggregate state is the same as period $t+1$ while the exogenous shocks are realized differently on the equilibrium path. We use $n_t^{(i)}$ as the endogenous aggregate state, as this is the only allocation that dynamically evolves. Specifically, we take the following steps:

3-1. Form a partition $\mathcal{P}^{\widetilde{A}}$ of the simulated path based on the aggregate productivity realizations.

$$\mathcal{P}^{\widetilde{A}} = \{\tau | A_\tau = \widetilde{A}\} \text{ for } \forall \widetilde{A} \in \mathcal{A}.$$

where $\mathcal{A}$ is the support (grids) of the productivity.

3-2. For each $\widetilde{A}$, find period $\tau^{\widetilde{A}} \in \mathcal{P}^{\widetilde{A}}$ such that the number of employed workers $n_\tau^{(i)}$ is identical (closest) to period $t+1$.[5]

$$\tau^{\widetilde{A}} = \arg\min_{\tau \in \mathcal{P}^{\widetilde{A}}} ||n_\tau^{(i)} - n_{t+1}^{(i)}||$$

3-3. Compute the rationally expected future variables using the allocations in period $\tau^{\widetilde{A}}$ for each $\widetilde{A}$. For example, the computation of Equation (1) is as follows:

$$RHS_t^{(i)} = \beta \sum_{\widetilde{A} \in \mathcal{A}} \Gamma_{A,\widetilde{A}} \left[(1 - H_{\tau^{\widetilde{A}}}^{(i)}) \left(\frac{c_{\tau^{\widetilde{A}}}^{(i)}}{c_t^{(i)}} \right)^{-\sigma} \left(\widetilde{A} \overline{Z}_{\tau^{\widetilde{A}}}^{(i)} - w_{\tau^{\widetilde{A}}}^{(i)} + (1-\lambda) \frac{\kappa}{q_{\tau^{\widetilde{A}}}^{(i)}} \right) \right].$$

where $\Gamma_{A,\widetilde{A}}$ is the transition probability of the aggregate productivity from a level A to a level $\widetilde{A}$.

[5] This step can be replaced by finding the closest period from above and the closest period from below. The detailed Explanation is in Lee (2025).

B Data, transformations and empirics

B.1 Data

We compute transition rates from IPUMS CPS micro data following Elsby, Hobijn, and Şahin (2015). Our sample consists of civilians aged 16–64; individuals are classified into E, U, and N using CPS employment-status codes, and adjacent months are linked using the CPS one-month longitudinal weight `lnkfw1mwt`. Short U–N–U and N–U–N "cycler" sequences are recoded so that the middle observation matches its neighbors (classification-error adjustment), and monthly transition probabilities p_{ij} are computed as the weighted fraction of persons in origin state i who are observed in destination state j in the following month. The resulting 3×3 transition matrices are then adjusted so that they map cross-sectional employment and unemployment stocks between t and $t+1$ (margin-error correction in the spirit of Abowd and Zellner (1985)). Before seasonal adjustment, outliers around the 1994 CPS redesign (1994–1996) are detected and replaced using `tsoutliers::tso`. Each flow series is then seasonally adjusted with X-13ARIMA-SEATS via the `seasonal` package Sax and Eddelbuettel (2018), applied to monthly data with at least two years of observations and with internal gaps linearly interpolated. Figure B.1 shows the resulting seasonally adjusted transition probabilities by origin labor market state.

Figure B.1: Transition rates between labor market states.

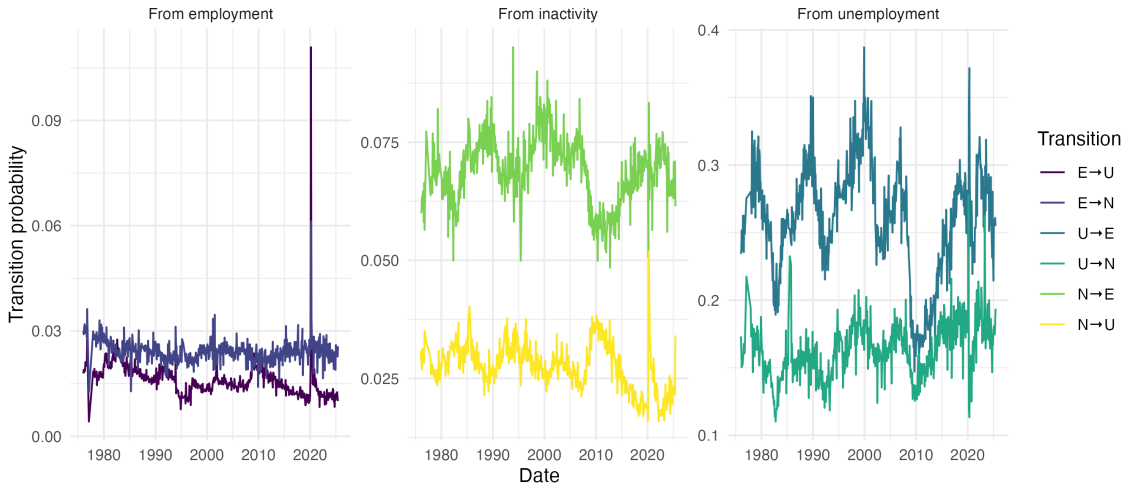

Notes: The panels plot seasonally adjusted monthly transition probabilities between employment (E), unemployment (U), and inactivity (N) constructed from IPUMS CPS micro data following Elsby, Hobijn, and Şahin (2015).

B.2 Measuring matching efficiency: Ahn and Crane (2020)

As in Ahn and Crane (2020), we assume a Cobb–Douglas matching function of the form $M_t = \mu_t U_t^{\sigma} V_t^{1-\sigma}$, where M_t denotes matches (hires), U_t unemployment, V_t vacancies, and μ_t captures (time-varying) matching efficiency. Dividing by unemployment yields a job-finding equation for the unemployed, $f_t = M_t/U_t$, which implies $\ln f_t = \ln \mu_t + (1-\sigma)\ln(\theta_t)$, where $\theta_t = V_t/U_t$ is labor market tightness. Writing $\ln \mu_t = \ln \bar{\mu} + \varepsilon_t$ gives the empirical specification $\ln f_t = \ln \bar{\mu} + \alpha \ln(\theta_t) + \varepsilon_t$, with $\alpha = 1 - \sigma$. Time variation in matching efficiency is then summarized by the fitted residual ε_t.

We implement this idea for two related series. Our *baseline* matching-efficiency series uses the CPS job-finding probability of the unemployed as the dependent variable f_t and defines tightness as vacancies per unemployed, $\theta_t = v_t/u_t$. Our *effective-searcher* series instead uses a generalized job-filling rate that averages transitions from unemployment and inactivity into employment using labor-force shares, and it

defines tightness as vacancies per effective searcher, $\theta_t^{\text{eff}} = v_t/\tilde{u}_t$, where $\tilde{u}_t$ denotes an effective-searcher measure combining unemployed and inactive workers (see the discussion in the main text). In both cases, we interpret the regression residual as a log matching-efficiency index; we use the baseline series in our main empirical analysis and the effective-searcher series in robustness checks.

Table B.1: Matching-function regressions for baseline and effective-searcher matching-efficiency series

	Specification	
Variable	**Baseline: log job-finding (U→E) on log tightness v_t/u_t**	**Effective-searcher: log generalized job-filling on log tightness $v_t/\tilde{u}_t$**
Constant	-1.127***	-2.257***
	(0.008)	(0.012)
Log tightness, $\log(\theta_t)$	0.244***	
	(0.011)	
Log generalized tightness, $\log(\theta_t^{\text{eff}})$		0.057***
		(0.010)

Note: Sample: Jan 1976 to Jun 2025. Data are monthly U.S. aggregates for employment, unemployment, vacancies, and CPS-based E–U–N transition probabilities. Column (1) regresses the log CPS job-finding rate of the unemployed on log labor market tightness $\theta_t = v_t/u_t$ (vacancies per unemployed); the residual from this regression defines our baseline matching-efficiency series. Column (2) regresses a generalized CPS job-filling rate, which averages transitions from unemployment and inactivity into employment using labor-force shares, on log generalized tightness $\theta_t^{\text{eff}} = v_t/\tilde{u}_t$, where $\tilde{u}_t$ is a measure of effective searchers combining unemployed and inactive workers. The residual from this regression defines the effective-searcher matching-efficiency series used in robustness checks. Standard errors are conventional OLS (i.i.d.). Significance levels: *** p<0.01, ** p<0.05, * p<0.10.

B.3 Derive approximate Beveridge curve dynamics

We start with the rewritten law of motion of employment,

$$v_t = M^{-1}(\frac{s_t}{1-s_t} - (u_{t+1} - u_t)\frac{1}{1-s_t}, m_t, u_t) \ . \tag{3}$$

First, we have to define the matching function. To keep tractability we assume a Cobb-Douglas Matching function, $M(m_t, v_t, u_t) = m_t v^{\alpha} u_t^{1-\alpha}$. Here $1-\alpha$ is the elasticity of the matching function to unemployment. Vacancies are then a function of the following equation,

$$v_t = (\frac{\frac{s_t}{1-s_t} - (u_{t+1} - u_t)\frac{1}{1-s_t}}{m_t u_t^{1-\alpha}})^{\frac{1}{\alpha}} \ . \tag{4}$$

We can then take logs and approximate each term around its steady state.

$$\ln(v_t) = \frac{1}{\alpha}[\ln(s_t - \Delta u_{t+1}) - \ln(1-s_t) - \ln(m_t) - (1-\alpha)\ln(u_t)] \ . \tag{5}$$

Note that Δu_{t+1} is 0 in steady state.

The first order approximation is then,

$$\frac{v_t - v}{v} \approx \frac{1}{\alpha}[\frac{s_t - s}{s} - \frac{u}{s}\frac{\Delta u_{t+1}}{u} + \frac{s}{1-s}\frac{s_t - s}{s} - \frac{m_t - m}{m} - (1-\alpha)\frac{u_t - u}{u}] \ . \tag{6}$$

We can collect terms and summarize each variable deviation as $\hat{x}_t = \frac{x_t - x}{x}$ which yields,

$$\hat{v} = \frac{v_t - v}{v} \approx \frac{1}{\alpha}[\frac{1}{1-s}\hat{s}_t - \frac{u}{s}\Delta\hat{u}_{t+1} - \hat{m}_t - (1-\alpha)\hat{u}_t] \ . \tag{7}$$

Parameterising this equation and adding deterministic components to control for these in the data yields,

$$\hat{v}_t = \beta_c + \beta_t t + \beta_u \hat{u}_t + \beta_m \hat{m}_t + \beta_s \hat{s}_t + \beta_{\Delta_u}\Delta\hat{u}_{t+1} + e_t, \tag{8}$$

Figure B.2: Derived log Separations, Matching efficiency, and Beveridge Curve shifts in Levels.

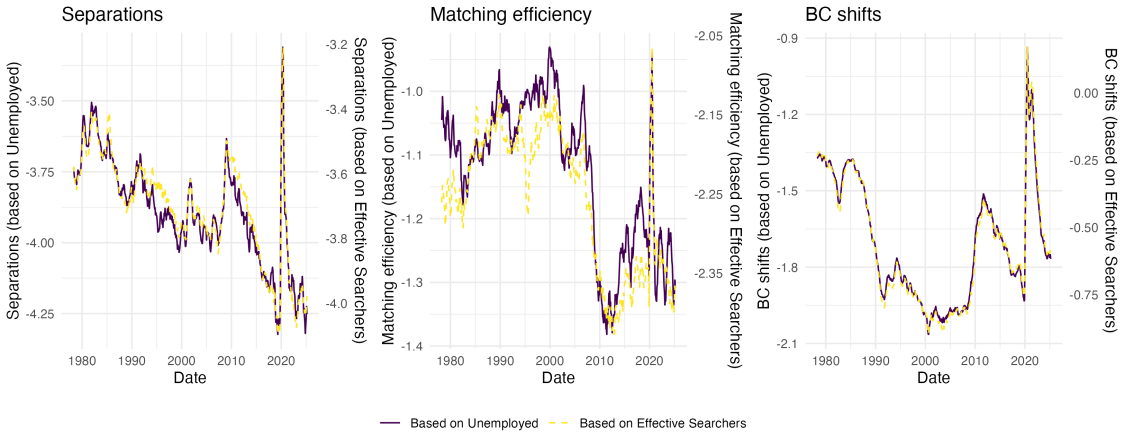

B.4 First-stage regression: Matching efficiency decomposition

Table B.2: First-stage regression: Matching efficiency on separations

	Matching Efficiency
Separations	0.092
	(0.022)
p_{UN}	0.438
	(0.130)
p_{NU}	0.498
	(0.594)
p_{EN}	3.373
	(1.172)
p_{NE}	4.120
	(0.569)
Constant	-0.460
	(0.052)
Observations	570

Note: Monthly U.S. data from January 1978 to June 2025. The dependent variable is matching efficiency. This first-stage regression generates the residual (orthogonalized matching efficiency) used in the channels decomposition reported in Table 3. The fitted values capture the endogenous separation channel, while the residuals capture the direct matching effect orthogonal to separations. Controls include CPS inactivity-flow transitions: p_{UN} (unemployment to inactivity), p_{NU} (inactivity to unemployment), p_{EN} (employment to inactivity), and p_{NE} (inactivity to employment). Standard errors are conventional i.i.d. OLS standard errors.

B.5 Robustness

Table B.3: Beveridge curve shifts, matching efficiency, and job separation (HP filter)

	Beveridge Curve Shifts		Beveridge Curve Shifts when ME $\geq$ 67th pctile(ME)	
	(1) Matching Efficiency	(2) Channels	(3) Matching Efficiency	(4) Channels
Matching Efficiency	-0.069		0.360	
	(0.082)		(0.095)	
Separations		0.849		0.412
		(0.045)		(0.082)
Matching Efficiency orthogonalized to Separations		-0.324		0.138
		(0.065)		(0.103)
Constant	-0.355	0.168	-0.144	-0.003
	(0.065)	(0.055)	(0.064)	(0.075)
Observations	570	570	190	190

Note: Monthly U.S. data from January 1978 to June 2025. The dependent variable is the Beveridge curve shift. This table replicates the analysis in Table 3 using Hodrick–Prescott (Hodrick and Prescott, 1997) filter detrending instead of the Rotemberg (Rotemberg, 1999) filter. Columns (1) and (3) report regressions of BC shifts on matching efficiency. Columns (2) and (4) report the channels decomposition: BC shifts regressed on separations and matching efficiency orthogonalized to separations. Columns (1)–(2) use the full sample, while columns (3)–(4) restrict to periods when matching efficiency (ME) exceeds the 67th percentile. All variables are standardized. The decomposition is implemented via a first-stage regression of matching efficiency on separations (including CPS inactivity-flow controls), with the fitted values capturing the endogenous separation channel and the residuals capturing the orthogonalized matching efficiency channel. The second-stage regressions control for log unemployment and CPS inactivity-flow transitions (p_{UN}, p_{NU}, p_{EN}, p_{NE}); coefficients on these controls are suppressed. Standard errors are conventional i.i.d. OLS standard errors.

C Wage bargaining in the baseline model

Real values of employment and unemployment We specify the value of employment with productivity z and wage w, $\widetilde{v}^e = \widetilde{v}^e(z, w; S)$ as follows:

$$\begin{aligned}
&\widetilde{v}^e(z, w; S) = w \\
&+ ((1-\lambda) + \lambda p(\theta(S)))\mathbb{E}\left[\mu(S, S')(1 - H(S'))(v^e(z'; S') - v^u(z'; S'))\middle| J(z'; S') > 0\right] \\
&+ \mathbb{E}\left[v^u(z'; S')\right] \qquad (9)
\end{aligned}$$

In equilibrium, the wage is determined by Nash bargaining, resulting in $w = w(z; S)$. We define the value function of an employed worker earning the equilibrium wage $v^e(z; S) := \widetilde{v}^e(z; S)(z, w(z; S); S)$ and the value function of an unemployed worker $v^u = v^u(z; S)$ as follows:

$$\begin{aligned}
&v^e(z; S) = w(z; S) \\
&+ ((1-\lambda) + \lambda p(\theta(S)))\mathbb{E}\left[\mu(S, S')(1 - H(S'))(v^e(z'; S') - v^u(z'; S'))\middle| J(z'; S') > 0\right] \\
&+ \mathbb{E}\left[\mu(S, S')v^u(z'; S')\right] \qquad (10) \\
&v^u(z; S) = b + p(\theta(S))\mathbb{E}\left[\mu(S, S')(1 - H(S'))(v^e(z, w'; S') - v^u(z'; S'))\middle| J(z'; S') > 0\right] \\
&+ \mathbb{E}\left[\mu(S, S')v^u(z'; S')\right] \qquad (11)
\end{aligned}$$

When a worker starts a period as unemployed, the worker engages in home production $b > 0$ and searches for a job to be matched with a vacancy with the probability $p = p(\theta(S))$.

Firms (=jobs) We specify the value function of a firm that is matched with a worker with productivity z and a wage level w:

$$\widetilde{J}(z, w; S) = Az - w + (1-\lambda)\mathbb{E}\left[\mu(S, S')(1 - H(S'))J(z'; S')|J(z'; S') > 0\right]. \qquad (12)$$

In equilibrium, the wage is determined as $w = w(z; S)$ by Nash bargaining. Based on this, we define the value function J of a firm that pays out the equilibrium wage, $J(z; S) = \widetilde{J}(z, w(z; S); S)$:

$$J(z; S) = Az - w(z; S) + (1 - \lambda)\mathbb{E}\left[\mu(S, S')(1 - H(S'))J(z'; S')|J(z'; S') > 0\right] \quad (13)$$

Wage bargaining A matched worker with productivity z and the firm determine the wage by Nash bargaining. The worker's bargaining power is η. The worker's benefit out of employment at wage w is $\widetilde{v}^e(z, w; S)$, and the outside option value is $v^u(z; S)$. The firms' benefit out of employing the worker at wage w is $\widetilde{J}(z, w; S)$, and the outside option is 0. This setup characterizes the following Nash bargaining:

$$w(z; S) = \arg\max_w \ (\widetilde{v}^e(z, w; S) - v^u(z; S))^\eta \left(\widetilde{J}(z, w; S)\right)^{1-\eta} \quad (14)$$

Then, from the optimality condition, we obtain the following condition:

$$(1 - \eta)(v^e(z; S) - v^u(z; S)) = \eta J(z; S) \quad (15)$$

D Job creation, destruction, and matching efficiency

We show here the static consequences of matching efficiency changes to Job Creation, Job Destruction and the Beveridge Curve.

In the spirit of Pissarides (2009), chapter 2 we describe the effect of matching efficiency variations on the job destruction cutoff. Job creation and job destruction contribute to the cutoff condition, which drives separation in our model. We show that only the job creation condition is affected by matching efficiency variations.

Definition 1 (Job Creation curve)**.**

Firms create jobs until the expected cost $\frac{\kappa}{q(\theta(S),)}$ *of a new job match equals the present discounted benefit the match,* $\frac{\kappa}{q(\theta(S),)} = (1-\lambda)\sum_{i=0}^{\infty}\mathbb{E}\left[\mu(S,S')(1-H(S'))J(z';S')|J(z';S')>0\right]$.

Iterating the equation forward yields in steady state,

$$\frac{\kappa}{q(m,\theta)} = \frac{(1-\eta)[\bar{z}(z_s^C)-b]-\eta\kappa\theta}{[\frac{1}{\beta(1-\lambda)(1-H(z_s^C))}-1]} \ . \tag{16}$$

Proposition 1 (The job creation curve)**.**
In the steady state, $z_s^C(S)$ *decreases in* θ*, ceteris paribus.*

Definition 2 (Job Destruction Curve)**.**
Firm-Worker matches dissolve when the benefit of the match to the firm falls below 0.This defines the cutoff point, $z_s = b+\frac{\eta}{1-\eta}\kappa-\frac{1}{1-\eta}(1-\lambda)\sum_{i=1}^{\infty}\mathbb{E}\left[\mu(S,S')(1-H(S'))J(z';S')|J(z';S')>\right.$

The endogenous job separation cutoff z_s^D is determined at the productivity level where a firm value becomes zero.

$$z_s^D(S) := \arg_z\{J(z;S)=0\} \tag{17}$$

In steady state this yields,

$$z_s^D = b+\frac{\eta}{1-\eta}\kappa-\frac{1}{1-\eta}\frac{(1-\eta)[\bar{z}(z_s)-b]-\eta\kappa\theta}{[\frac{1}{\beta(1-\lambda)(1-H(z_s^D))}-1]} \ . \tag{18}$$

Note that matching efficiency does not enter the job destruction condition. Further, tightness θ can be isolated from z_s^D. It then is clear that the next proposition holds.

Proposition 2 (The job destruction curve)**.**
In the steady state, $z_s^D(S)$ *increases in* θ*, ceteris paribus.*

Proof. The result is immediate from Equation (18). ■

Figure D.3: The job creation (JC) and job destruction condition (JD), with different matching efficiencies.

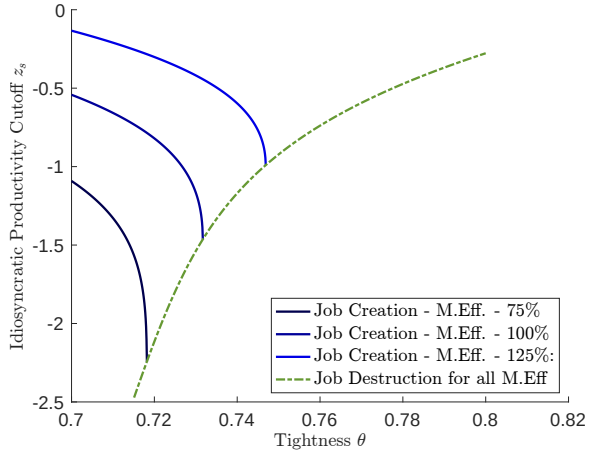

When the matched job value function J is recursively expressed, it is as follows:

$$z_s^D(S) = \frac{(1-\eta)b + \eta\theta\kappa - \mathcal{W}}{(1-\eta)A} \tag{19}$$

$$\mathcal{W} = \sum_{n=0}^{\infty}(1-\lambda)^n \mathbb{E}[\mu(S, S^{(n)})(1 - H(S^{(n)}))((1-\eta)(Az^{(n)} - b) - \eta\theta^{(n)}\kappa | J(z^{(n)}; S^{(n)}) > 0] \tag{20}$$

From Equation (20), the sequential persistence in θ dynamically affects z_s^D through $\theta^{(n)}$, which is computationally handled in our global solution. In particular, a contemporaneous increase in matching efficiency does not directly affect reservation productivity z_s^D, implying that increase in matching efficiency does not shift the job destruction curve.

In the equilibrium, the reservation $z_s(S)$ is determined at $z_s^D(S) = z_s^C(S)$

E Extended baseline model with policy variables

Household We consider a representative household that is composed of a continuum of unit measures of labor forces. The employed portion of the labor force earns wages, and the unemployed portion engages in home production, all of which are

treated as labor income $W(S)$. The household holds the claim for the dividend $D(S)$ and saves for future dividend claims. Thus, the budget constraint is as follows:

$$c + a' = W(S) + D(S) + \underbrace{(a - D(S))}_{\text{Ex-dividend equity value}} - T(S) \tag{21}$$

where $T(S)$ is the lump-sum tax, and a is the value of the dividend claim. The apostrophe indicates the future variables. The household has a temporal CRRA utility and discounts future by $\beta \in (0, 1)$. The recursive formulation of the households' problem is as follows:

$$V(a; S) = \max_{c,a'} \quad \frac{c^{1-\sigma}}{1-\sigma} + \beta \mathbb{E} V(a'; S') \tag{22}$$

$$\text{s.t.} \quad c + a' = W(S) + D(S) + (a - D(S)) - T(S) \tag{23}$$

Real values of employment and unemployment A continuum of a unit measure of ex-ante heterogeneous labor force is considered. Their labor productivity z is distributed as follows:

$$z \sim N(0, \sigma_z) \tag{24}$$

When a worker is employed, they earn wage. Then, an exogenous Poisson separation shock arrives at a rate of $\lambda \in (0, 1)$. The worker continues to work in the following period with a probability of $(1 - \lambda)$ or searches for another job with probability λ and gets matched with a new job with a probability of $p = p(\theta(S))$.

$$\begin{aligned}
&\widetilde{v}^e(z, w; S) = w \\
&+ ((1 - \lambda) + \lambda p(\theta(S))) \mathbb{E}\left[\mu(S, S')(1 - H(S'))(v^e(z; S') - v^u(z; S')) \middle| J(z; S') > -\mathcal{F}_f(S')\right] \\
&+ \mathbb{E}\left[v^u(z; S')\right]
\end{aligned} \tag{25}$$

In the following period, a firm decides whether to lay off the worker, which is captured

by endogenous separation rate $H(S')$. All workers are assumed to participate in job search when unemployed. All the future values are discounted by the stochastic discount factor $\mu(S, S')$. Equation (25) characterizes the value of employment with productivity z and wage w, $\widetilde{v}^e = \widetilde{v}^e(z, w; S)$. In equilibrium, the wage is determined by Nash bargaining, resulting in $w = w(z; S)$. We define the value function of an employed worker earning the equilibrium wage $v^e(z; S) := \widetilde{v}^e(z; S)(z, w(z; S); S)$ and the value function of an unemployed worker $v^u = v^u(z; S)$ as follows:

$$
\begin{aligned}
&v^e(z; S) = w(z; S) \\
&+ ((1-\lambda) + \lambda p(\theta(S)))\mathbb{E}\left[\mu(S, S')(1 - H(S'))(v^e(z; S') - v^u(z; S'))\middle| J(z; S') > -\mathcal{F}_f(S')\right] \\
&+ \mathbb{E}\left[\mu(S, S')v^u(z; S')\right] \qquad (26) \\
&v^u(z; S) = b + p(\theta(S))\mathbb{E}\left[\mu(S, S')(1 - H(S'))(v^e(z, w'; S') - v^u(z; S'))\middle| J(z; S') > -\mathcal{F}_f(S')\right] \\
&+ \mathbb{E}\left[\mu(S, S')v^u(z; S')\right] \qquad (27)
\end{aligned}
$$

When a worker starts a period as unemployed, the worker engages in home production $b > 0$ and searches for a job to be matched with a vacancy with the probability $p = p(\theta(S))$.

Firms (=jobs) A firm (job) produces output using a CRS Cobb-Douglas function with only a labor input.[6] Equation (28) characterizes the value function of a firm that is matched with a worker with productivity z and a wage level w:

$$
\widetilde{J}(z, w; S) = Az - w + (1-\lambda)\mathbb{E}\left[\mu(S, S')(1 - H(S'))J(z; S')|J(z; S') > -\mathcal{F}_f(S')\right] \qquad (28)
$$

where $\mu(S, S')$ is the stochastic discount factor. In equilibrium, the wage is determined as $w = w(z; S)$ by Nash bargaining. Based on this, we define the value function J of

[6]The CRS production allows the firm-level characterization to boil down to the job-level characterization as in other models in the literature.

a firm that pays out the equilibrium wage, $J(z;S) = \widetilde{J}(z, w(z;S);S)$:

$$J(z;S) = Az - w(z;S) + (1-\lambda)\mathbb{E}\left[\mu(S,S')(1-H(S'))J(z;S')|J(z;S') > -\mathcal{F}_f(S')\right] \tag{29}$$

At the beginning of a period, a firm decides whether to destruct a job based on the following individual rationality condition: $J(z;S) > -\mathcal{F}_f(S')$. It is worth noting that all the value functions are written at the timing after the job destruction decision, which eases the wage bargaining characterization. We define the endogenous job destruction probability $H(S)$ accordingly:

$$H(S) := \mathbb{P}\left(J(z;S) < -\mathcal{F}_f(S')\right). \tag{30}$$

We allow $\mathcal{F}_f(S) < 0$, which captures the possibility of levying taxes for operating firms.

Wage bargaining A matched worker with productivity z and the firm determine the wage by Nash bargaining. The worker's bargaining power is η. The worker's benefit out of employment at wage w is $\widetilde{v}^e(z,w;S)$, and the outside option value is $v^u(z;S)$. The firms' benefit out of employing the worker at wage w is $\widetilde{J}(z,w;S)$, and the outside option is 0. This setup characterizes the following Nash bargaining:

$$w(z;S) = \arg\max_w \ \left(\widetilde{v}^e(z,w;S) - v^u(z;S)\right)^\eta \left(\widetilde{J}(z,w;S) + \mathcal{F}_f(S)\right)^{1-\eta} \tag{31}$$

Government Government determines the firing regulation $\mathcal{F}_f$. Depending on the sign of the regulation term, a lump-sum tax or a lump-sum subsidy is imposed for

the households.

$$T(S) = v(S)\mathcal{F}_h(S) - \underbrace{(1-\lambda)H(S)(n_{-1} + v(S)q(\theta(S)))}_{\text{Endogenously fired workers}}\mathcal{F}_f(S) \tag{32}$$

The lump-sum subsidy or tax is canceled out by the changes in the dividend, leading to a net zero effect on consumption.

Equilibrium conditions In equilibrium, we require the following conditions:

$$\begin{aligned}\text{[Free entry]} \quad & \kappa - \mathcal{F}_h(S) \\ & = q(\theta(S))(1-\lambda)\mathbb{E}\left[\mu(S,S')(1-H(S'))J(z;S')|J(z;S') > -\mathcal{F}_f(S')\right]\end{aligned} \tag{33}$$

$$\text{[Agg. output]} \quad Y(S) = A\int_{J(z;S)>-\mathcal{F}_f(S)} z d\Phi + b\int_{J(z;S)>-\mathcal{F}_f(S)} d\Phi \tag{34}$$

$$\text{[Resource const.]} \quad C(S) = Y(S) - \kappa v(S) = W(S) + D(S) - T(S) \tag{35}$$

The first is free entry conditions. Firms pay a cost κ when they post a vacancy. In equilibrium, a firm's expected profit and the vacancy posting cost balance. In the national account, aggregate output Y balances with the aggregate consumption C after accounting for the total vacancy posting cost. From the income side identity, the consumption is equal to the sum of labor and capital (dividend) incomes minus the lump-sum tax.

E.1 Equilibrium characterization

From the free entry condition, we derive

$$\widetilde{J}(z,w;S) = Az - w + \frac{\kappa - \mathcal{F}_h(S)}{q(\theta(S))}. \tag{36}$$

Therefore,

$$J(z;S) = Az - w(z;S) + \frac{\kappa - \mathcal{F}_h(S)}{q(\theta(S))}. \tag{37}$$

From the Nash bargaining, we have

$$(1-\eta)(v^e(z;S) - v^u(z;S)) = \eta(J(z;S) + \mathcal{F}_f(S)) \tag{38}$$

Combining (25) and (27) with (38), we obtain

$$\widetilde{v}^e(z,w;S) - v^u(z;S) = w - b + (1-p(\theta(S)))\frac{\eta}{1-\eta}\frac{\kappa - \mathcal{F}_h(S)}{q(\theta(S))} \tag{39}$$

$$= w - b + \frac{\eta}{1-\eta}\frac{\kappa - \mathcal{F}_h(S)}{q(\theta(S))} - \frac{\eta}{1-\eta}\theta(\kappa - \mathcal{F}_h(S)) \tag{40}$$

Thus, the Nash bargaining outcome becomes

$$(1-\eta)\left(w(z;S) - b + \frac{\eta}{1-\eta}\frac{\kappa - \mathcal{F}_h(S)}{q(\theta(S))} - \frac{\eta}{1-\eta}\theta(\kappa - \mathcal{F}_h(S))\right)$$
$$= \eta\left(Az - w(z;S) + \frac{\kappa - \mathcal{F}_h(S)}{q(\theta(S))} - \mathcal{F}_f(S)\right), \tag{41}$$

which leads to the following equilibrium wage characterization:

$$w(z;S) = (1-\eta)b + \eta(Az + \theta(\kappa - \mathcal{F}_h(S))) + \eta\mathcal{F}_f(S). \tag{42}$$

Due to the endogenous decision for the job destruction, there exists the productivity threshold $z_s = z_s(S)$ such that a firm becomes indifferent between keeping the

job and destruction:

$$z_s(S) := \arg_z\{J(z;S) = -\mathcal{F}_f(S)\} \iff J(z_s(S);S) = -\mathcal{F}_f(S). \tag{43}$$

$$\iff Az_s(S) - w(z_s(S);S) + \frac{\kappa - \mathcal{F}_h(S)}{q(\theta(S))} = -\mathcal{F}_f(S) \tag{44}$$

$$\iff (1-\eta)(Az_s(S) - b) - \eta\theta(\kappa - \mathcal{F}_h(S)) - \eta\mathcal{F}_f(S) + \frac{\kappa - \mathcal{F}_h(S)}{q(\theta(S))} = -\mathcal{F}_f(S) \tag{45}$$

$$\iff z_s(S) = \frac{1}{A}\left(b + \frac{\eta}{1-\eta}\theta(\kappa - \mathcal{F}_h(S)) - \frac{1}{1-\eta}\frac{\kappa - \mathcal{F}_h(S)}{q(\theta(S))} - \mathcal{F}_f(S)\right) \tag{46}$$

Based on this threshold, we characterize the following endogenous separation probability:

$$H(S) := \mathbb{P}(J(z;S) < -\mathcal{F}_f(S)) = \mathbb{P}(z < z_s(S)) = \Phi\left(\frac{z_s(S) - 1}{\sigma_z}\right) \tag{47}$$

The conditional average productivity of employed workers $\overline{z} = \overline{z}(S)$ is as follows:

$$\overline{z}(S) := \mathbb{E}\left[z\middle|J(z;S) > -\mathcal{F}_f(S)\right] = \mathbb{E}\left[z\middle|z > z_s(S)\right] \tag{48}$$

$$= 1 + \sigma_z \frac{\phi(\frac{z_s(S)-1}{\sigma_z})}{1 - \Phi(\frac{z_s(S)-1}{\sigma_z})} \tag{49}$$

Similarly, the conditional average wage of employed workers $\overline{w} = \overline{w}(S)$ is as follows:

$$\overline{w}(S) := \mathbb{E}\left[w(z;S)\middle|J(z;S) > -\mathcal{F}_f(S)\right] \tag{50}$$

$$= (1-\eta)b + \eta(A\overline{z} + \theta(\kappa - \mathcal{F}_h(S))) + \eta\mathcal{F}_f(S). \tag{51}$$

Using these conditional averages, we can characterize the following job creation con-

dition from (33) and (37):

$$\frac{\kappa - \mathcal{F}_h(S)}{q(\theta(S))} = (1-\lambda)\mathbb{E}\left[\mu(S,S')(1-H(S'))J(z;S')|J(z;S') > -\mathcal{F}_f(S')\right] \tag{52}$$

$$= (1-\lambda)\mathbb{E}\left[\mu(S,S')(1-H(S'))\left(A\overline{z}(S') - \overline{w}(S') + \frac{\kappa - \mathcal{F}_h(S')}{q(\theta(S'))}\right)\right] \tag{53}$$

$$= (1-\lambda)\mathbb{E}\left[\mu(S,S')(1-H(S'))\left((1-\eta)(A\overline{z}(S') - b) - \eta\theta(\kappa - \mathcal{F}_h(S'))\right.\right. \tag{54}$$

$$\left.\left. -\eta\mathcal{F}_f(S') + \frac{\kappa - \mathcal{F}_h(S')}{q(\theta(S'))}\right)\right]. \tag{55}$$

Table E.4 summarizes the set of assumptions and the equilibrium conditions of the baseline model.

Table E.4: Summary of assumptions and the equilibrium conditions with policy variables

Description	**Equation**
Aggregate productivity	$\ln(A') = \rho_A \ln(A) + \sigma_A \epsilon$
Aggregate matching efficiency	$\ln(m') = \rho_m \ln(m) + \sigma_m \epsilon$
Endogenous Job destruction	$H = \Phi(\frac{z_s - 1}{\sigma_z})$
Law of motion of employment	$n = (1-\lambda)(1-H)n_{-1}^*$
Job creation condition	$\frac{\kappa - \mathcal{F}_h}{q(\theta)} = (1-\lambda)\mathbb{E}[\mu(1-H')\left(A'\overline{z}' - \overline{w}' + \frac{\kappa - \mathcal{F}_h'}{q(\theta')}\right)]$
Job destruction condition	$Az_s = b + \frac{\eta}{1-\eta}(\kappa - \mathcal{F}_h)\theta - \frac{1}{1-\eta}\frac{\kappa - \mathcal{F}_h}{q(\theta)} - \mathcal{F}_f$
Cond. mean match productivity	$\overline{z} = 1 + \sigma_z \frac{\phi(\frac{z_s-1}{\sigma_z})}{1-\Phi(\frac{z_s-1}{\sigma_z})}$
Bargained average wage	$\overline{w} = (1-\eta)b + \eta[A\overline{z} + \theta(\kappa - \mathcal{F}_h)] + \eta\mathcal{F}_f(S)$
Probability of finding a job	$p(\theta) = m\theta(1+\theta^\xi)^{-\frac{1}{\xi}}$
Probability of filling a vacancy	$q(\theta) = m(1+\theta^\xi)^{-\frac{1}{\xi}}$
Resource constraint	$C = A\overline{z}n + b(1-n) - \kappa v$
Stochastic discount factor	$\mu = \beta\left(\frac{C'}{C}\right)^{-\sigma}$
Government budget balance	$T = v\mathcal{F}_h - (1-\lambda)Hn_{-1}^*\mathcal{F}_f$
Tightness	$\theta = \frac{v}{u}$
Unemployed	$u = 1 - n$

F Dynamic implications of the Beveridge curve

The Beveridge curve captures the relationship between the contemporaneous unemployment and vacancy posting rates. However, the dynamic implications of the Beveridge curve are relatively less investigated in the literature. We mainly focus on how a high/low vacancy posting rate affects the future unemployment dynamics. All the allocations are obtained from the simulated path of 30,000 periods (months) based on the global solution.

Figure F.4 plots the histograms of the future unemployment rates conditional on the high (dark color) and low (bright color) contemporaneous vacancy posting rates and the high (panel (a)) and low (panel (b)) contemporaneous unemployment rates. The vertical dash-dotted and dashed lines are the average future unemployment rates for high and low contemporaneous vacancy postings.

The high unemployment period is with unemployment rates greater than 8% and lower than 10%. The low unemployment period is with unemployment rates greater than 3% and lower than 5%. The high vacancy period is with vacancy posting rates greater than 80^{th} quantile (around 5.5%). The low vacancy period is with vacancy posting rates lower than 20^{th} quantile (around 2.7%).[7] The average contemporaneous unemployment rates of high and low vacancy periods are 8.26% and 8.73% for high unemployment periods (panel (a)) and 4.17% and 4.14 % for low unemployment periods (panel (b)). The average future unemployment rates of high and low vacancy periods are 7.76% and 8.80% for high unemployment periods (panel (a)) and 4.16% and 4.18 % for low unemployment periods (panel (b)).

When a high unemployment rate is observed, the future unemployment is sub-

[7]For the unemployment rate cutoffs, we alternatively define high unemployment period with unemployment rates greater than 80^{th} quantile (around 7.2%) and low unemployment period with unemployment rates lower than 20^{th} quantile (around 4.0%). The result stays unchanged by this choice. However, the average contemporaneous unemployment rates become significantly different between the high and low vacancy periods, which disturbs a fair comparison of future unemployment rates; it is natural that contemporaneously different unemployment rates lead to different future rates.

Figure F.4: Conditional Distribution of the future unemployment rate

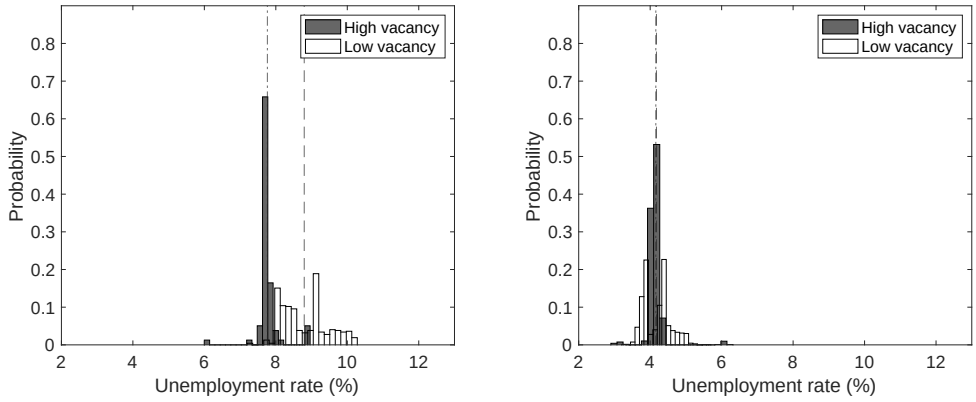

(a) High u_t (b) Low u_t

stantially differently realized depending on the contemporaneous vacancy rate level. On the other hand, this future unemployment dependence on the vacancy rate disappears in the low unemployment periods. When the unemployment rate is high, and the vacancy posting rate is low, the future unemployment rate is likely to stay at a higher level than the periods with low vacancy posting rates.

We extend this analysis of one-period future unemployment to extended future periods. Figure F.5 plots the time-series average of the conditional dynamic stochastic unemployment rate path with the 95% confidence interval. When a high unemployment rate is observed, depending on the level of contemporaneous vacancy posting rate, the future paths of unemployment rates are significantly different. When the vacancy posting rate is low, the economy's unemployment rate stays persistently higher (dashed line in panel (a)) than the other (solid line in panel (a)). On the other hand, the conditional unemployment path does not significantly depend on the vacancy posting rate when a low unemployment rate is observed (panel (b)).

G State-dependent responsiveness: Other variables

Figure F.5: Conditional dynamics of the unemployment rate

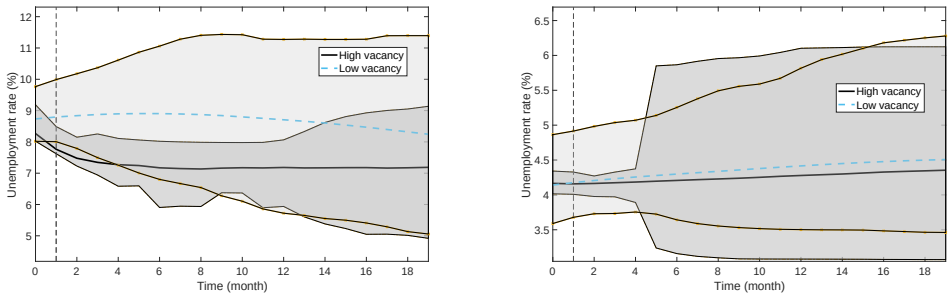

(a) High u_t (b) Low u_t

Table G.5: State-dependent shock responsiveness of unemployment rate

	Dependent variable: u_t (%)			
	Model		Data	
TFP_t (%)	-5.878	0.353	-1.7	- 6.9
	(0.041)	(0.008)	(0.37)	(2.98)
$TFP_t \times (1 - n^*_{t-1})$ (%)		0.226		0.88
		(0.004)		(0.49)
m_t (%)	4.168	2.902	9.68	10.8
	(0.063)	(0.012)	(0.029)	(3.01)
$m_t \times (1 - n^*_{t-1})$ (%)		0.023		1.08
		(0.003)		(2.75)
Constant	Yes	Yes	Yes	Yes
Observations	15,000	15,000	84	83
R^2	0.642	0.994	0.7485	
Adjusted R^2	0.642	0.994		

Figure G.6: The nonlinear state-dependent responsiveness to TFP variations

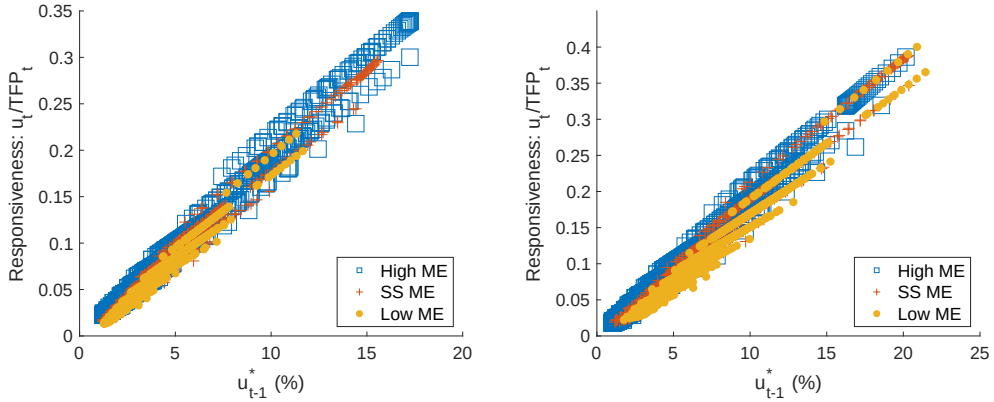

(a) u_t/TFP_t and u^*_{t-1}: baseline (b) u_t/TFP_t and u^*_{t-1}: exo. separation

Notes: u^*_{t-1} is defined as $u_{t-1} := 1 - n^*_{t-1}$.

Figure G.7: The nonlinear state-dependent responsiveness to TFP variations

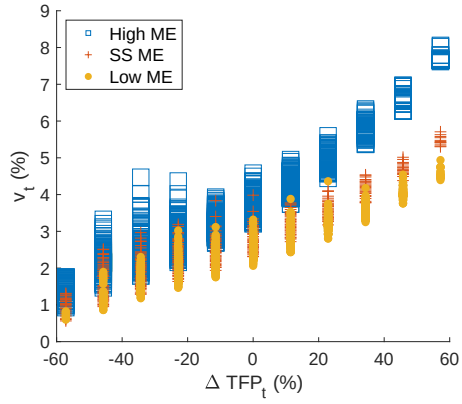

(a) TFP_t and v_t: baseline

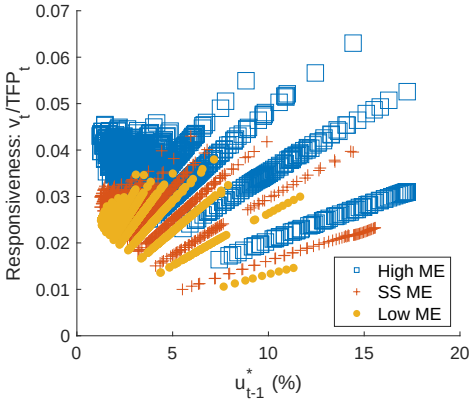

(b) v_t/TFP_t and u^*_{t-1}: baseline

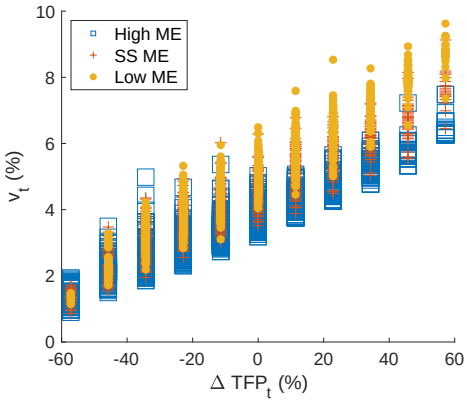

(c) TFP_t and v_t: exo. separation

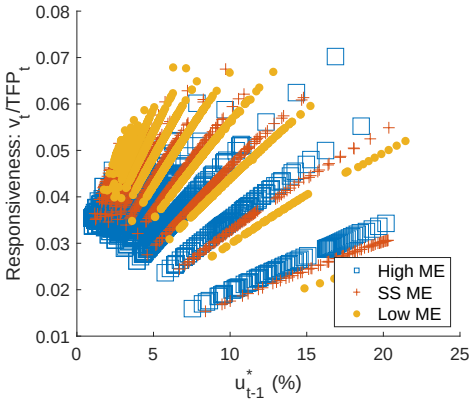

(d) v_t/TFP_t and u^*_{t-1}: exo. separation

Notes: u^*_{t-1} is defined as $u_{t-1} := 1 - n^*_{t-1}$.

Figure G.8: The nonlinear state-dependent responsiveness to TFP variations

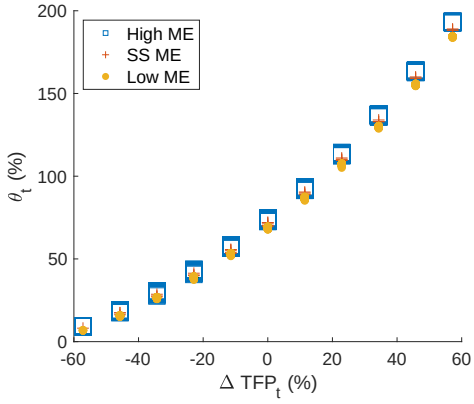

(a) TFP_t and θ_t: baseline

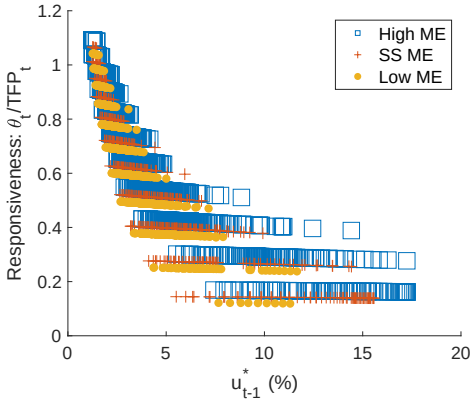

(b) θ_t/TFP_t and u^*_{t-1}: baseline

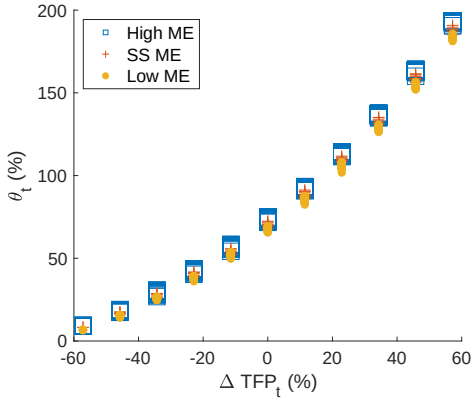

(c) TFP_t and θ_t: exo. separation

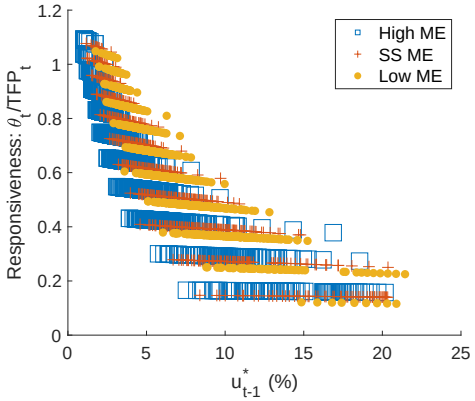

(d) θ_t/TFP_t and u^*_{t-1}: exo. separation

Notes: u^*_{t-1} is defined as $u_{t-1} := 1 - n^*_{t-1}$.

Figure G.9: The nonlinear state-dependent responsiveness to TFP variations

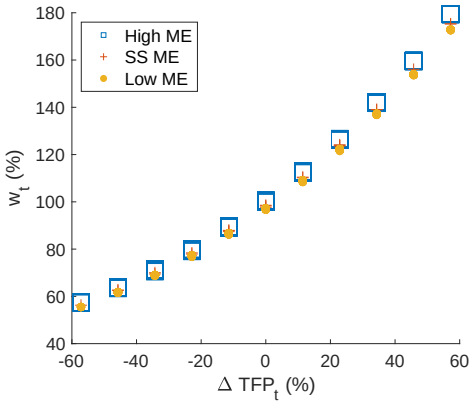

(a) TFP_t and w_t: baseline

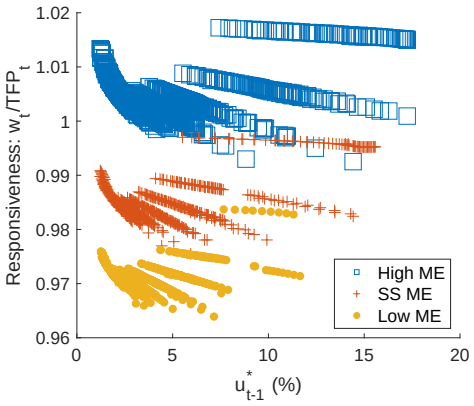

(b) w_t/TFP_t and u^*_{t-1}: baseline

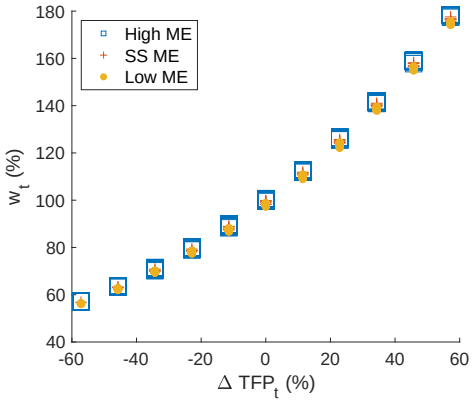

(c) TFP_t and w_t: exo. separation

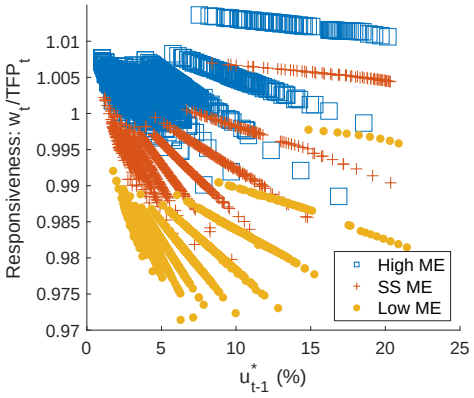

(d) w_t/TFP_t and u^*_{t-1}: exo. separation

Notes: u^*_{t-1} is defined as $u_{t-1} := 1 - n^*_{t-1}$.

H Hosios-implied efficiency

Figure H.10: The Beveridge curves: Hosios vs. Baseline

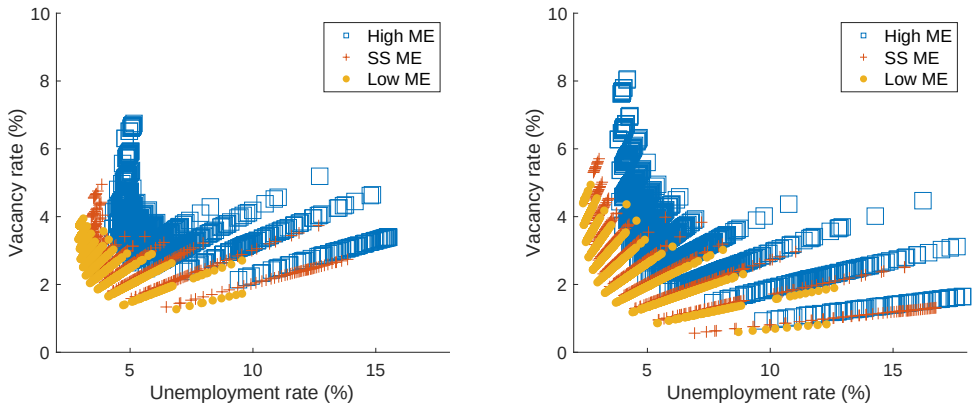

(a) Hosios (b) Baseline

Figure H.10 plots the equilibrium Beveridge curves of the Hosios-efficient model (panel (a)) and the baseline model (panel (b)). Reflecting the dampened volatilities of the unemployment and the vacancy posting, the Beveridge curve display narrower variation along the two axes compared to the baseline model. We use the Hosios-efficient equilibrium allocations as one benchmark for our policy discussion in the following sections.

I Policy analysis

I.1 Optimal firing penalty policy

In this section, we study the optimal firing penalty(subsidy) policy with respect to the equilibrium unemployment dynamics. Particularly, we focus on the constant firing penalty policy $\mathcal{F}_f$, assuming that the policy is not frequently adjustable over the business cycle. When $\mathcal{F}_f < 0$, the corresponding policy is a firing subsidy, which is equivalent to a tax to an operating job (firm) in our setup. We label this policy as the corporate tax. Depending on the policy parameter level and the sign,

the endogenous job destruction, bargaining outcome, and vacancy posting conditions are significantly affected, leading to variations in the unconditional unemployment average and volatility.

Figure I.11: The optimal vacancy posting subsidy

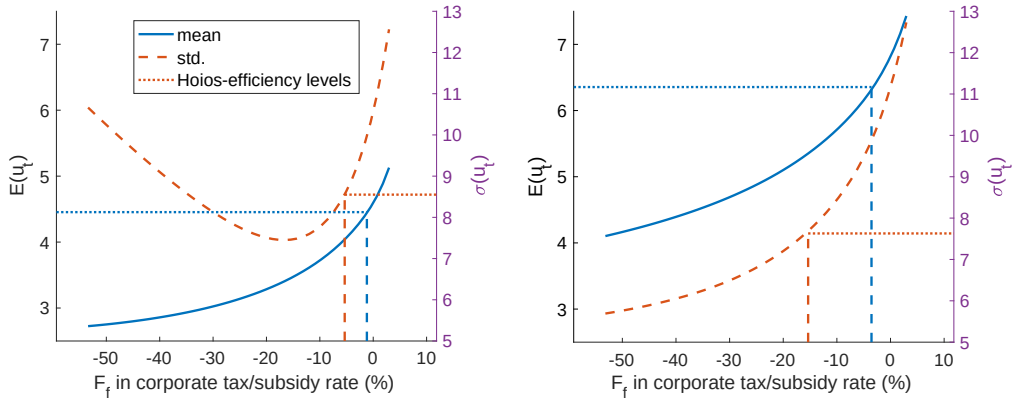

(a) Baseline (b) Exogenous separation

Figure I.11 compares the unconditional unemployment mean and volatility variations over the policy parameter change for the baseline model (panel (a)) and for the exogenous separation model (panel (b)). The baseline model with the endogenous separation shows a stark trade-off between the mean and volatility when the corporate tax rate increases (a negatively larger $\mathcal{F}_f$) after a threshold level, while the exogenous separation model does not feature this trade-off. Notably, the Hosios-efficient mean and volatilities are not jointly achievable by the single policy variation in $\mathcal{F}_f$. Therefore, depending on the government's description, the optimal policy is suboptimally determined.

I.2 Covid-19 and optimal firing policy

I.3 Optimal vacancy posting subsidy

In this section, we analyze the optimal vacancy posting subsidy that perfectly achieves the Hosios-efficient vacancy posting dynamics. This policy analysis is hypothetical,

Figure I.12: The optimal policy and other variables' responses

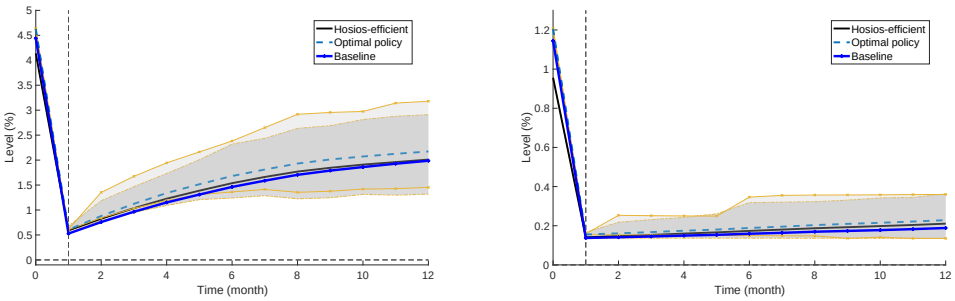

(a) Vacancy (v_t) (b) Market tightness (θ_t)

as we allow the vacancy posting subsidy to fluctuate period-by-period, which is infeasible in reality. However, the analysis is meaningful in showing the existence of the optimal counter-cyclical subsidy plan and in analyzing the policy's macroeconomic implications.

Figure I.13: The optimal vacancy posting subsidy

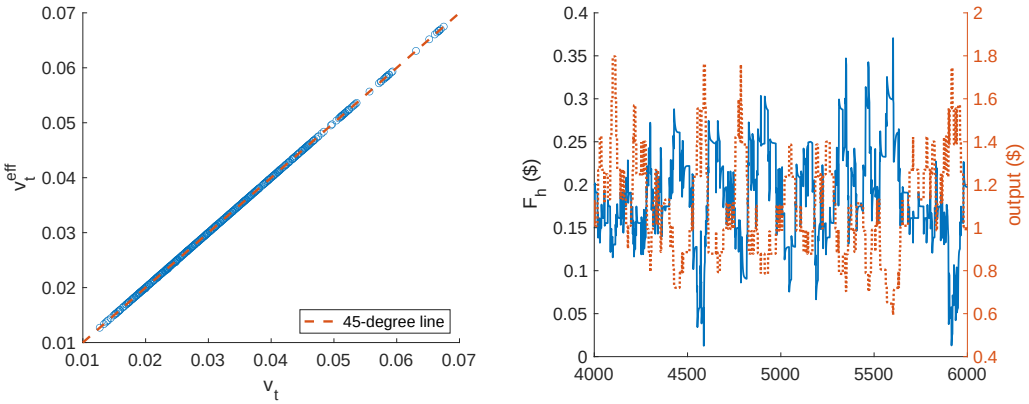

(a) Optimality check for the policy $\mathcal{F}_h$ (b) Time series of optimal subsidy $\mathcal{F}_h$

Figure I.13 shows the optimality of the policy we compute based on the global nonlinear solution. Panel (a) is a scatter plot of vacancy posting under the optimal $\{\mathcal{F}_f\}_{t=0}^{T}$ in the horizontal axis and the Hosios-efficient vacancy postings in the vertical axis. The scatter plot is perfectly aligned with the 45-degree line, which verifies the optimality of the policy. Panel (b) shows the time series of the optimal policy in

comparison to the aggregate output. The optimal vacancy posting subsidy is sharply counter-cyclical, featuring the correlation coefficient with output at -0.91.

Figure I.14: Economy with optimal vacancy subsidy vs. Baseline

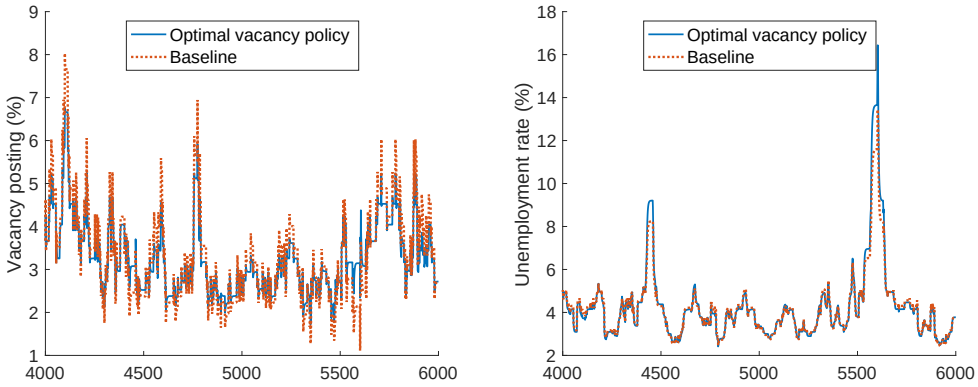

(a) Vacancy (b) Unemployment

The optimal policy successfully recovers the optimal vacancy posting fluctuations. However, it is sub-optimal with respect to the unemployment dynamics. Figure I.14 shows that the reduced vacancy posting volatility (panel (a)) backfires through the heightened unemployment volatility (panel (b)), marking the unemployment volatility at 11.30%. This backfire is through the endogenous job separation channel, which is necessarily not captured by the model with exogenous job separation.

J Proofs

Proposition 3 (The shape of the elasticity)**.**

The elasticity of the separation to the matching efficiency change is hump-shaped:

$$\lim_{m\to 0} \frac{\partial}{\partial m} \frac{\partial log(s(m))}{\partial log(m)} = 0, \quad \lim_{m\to \infty} \frac{\partial}{\partial m} \frac{\partial log(s(m))}{\partial log(m)} = \infty, \tag{56}$$

and $lim_{m\to\infty} \frac{\partial}{\partial m} \frac{\partial log(s(m))}{\partial log(m)}$ *flips the sign only once.*

Proof.

Let $\lambda \in (0,1)$, $D > 0$, and $A \in \mathbb{R}$ be arbitrary constants. Define

$$u(m) = A - \frac{D}{m}, \qquad \Phi(u) = \int_{-\infty}^{u} \phi(t)\, dt,$$

where $\phi(u) = \frac{1}{\sqrt{2\pi}} e^{-u^2/2}$ is the standard normal density and Φ its CDF. Then

$$s(m) = \lambda + (1-\lambda)\, \Phi\big(u(m)\big), \qquad E(m) = \frac{\partial \ln s(m)}{\partial \ln m} = \frac{m}{s(m)}\, \frac{ds}{dm}.$$

A direct differentiation shows

$$s'(m) = (1-\lambda)\, \phi\big(u(m)\big)\, \frac{D}{m^2}, \quad E(m) = \frac{(1-\lambda)\, D}{m\, s(m)}\, \phi\big(u(m)\big).$$

i) Limits at the Boundaries

1. $m \to 0^+$:

   $$u(m) = A - \frac{D}{m} \to -\infty \quad \Longrightarrow \quad \phi(u(m)) \to 0 \quad \text{(super-exponentially)}, \quad s(m) \to \lambda > 0,$$

   hence $0 \le E(m) \to 0$.

2. $m \to +\infty$:

   $$u(m) \to A, \quad s(m) \to \lambda + (1-\lambda)\Phi(A) > 0,$$

   but the prefactor $1/m$ drives $E(m) \sim \dfrac{\text{const}}{m} \to 0$.

Thus

$$\lim_{m \to 0^+} E(m) = 0, \quad \lim_{m \to \infty} E(m) = 0.$$

ii) Positivity of $E(m)$

Since $(1-\lambda), D, m, s(m), \phi(u(m))$ are all strictly positive on $(0, \infty)$, we have

$$E(m) = \frac{(1-\lambda)\, D}{m\, s(m)}\, \phi\big(u(m)\big) > 0 \quad \forall\, m > 0.$$

iii) Existence and Uniqueness of the Peak

Define the log-elasticity

$$L(m) = \ln E(m) = \ln\big[(1-\lambda)D\big] - \ln m - \ln s(m) + \ln \phi\big(u(m)\big).$$

Differentiate term by term:

$$\frac{dL}{dm} = -\frac{1}{m} - \frac{s'(m)}{s(m)} + \frac{\phi'(u(m))}{\phi(u(m))}\, u'(m).$$

Using $s'(m)/s(m) = E(m)/m$, $\phi'(u) = -u\,\phi(u)$, and $u'(m) = D/m^2$, we obtain

$$\frac{dL}{dm} = -\frac{1}{m} - \frac{E(m)}{m} - u(m)\,\frac{D}{m^2} = \frac{-1 - E(m) - \frac{D}{m}u(m)}{m}.$$

Since $m > 0$, the sign of $E'(m)$ coincides with the sign of

$$f(m) = -1 - E(m) - \frac{D}{m}\,u(m).$$

iiia) Endpoint Signs of $f(m)$

- As $m \to 0^+$, $u(m) \to -\infty$ so $-\frac{D}{m}u(m) \to +\infty$, and $-1 - E(m)$ remains bounded. Therefore $f(m) \to +\infty$ and $E'(m) > 0$ for small m.
- As $m \to \infty$, $u(m) \to A$, $E(m) \to 0$, so $f(m) \to -1 < 0$ and $E'(m) < 0$ for large m.

iiib) Monotonicity of $f(m)$

A straightforward (albeit tedious) calculation shows

$$f'(m) < 0 \quad \forall\, m > 0.$$

Hence f is strictly decreasing from $+\infty$ to -1, crossing zero exactly once. Denote

this unique root by m^*. Then

$$E'(m) > 0 \ (m < m^*), \quad E'(m) = 0 \ (m = m^*), \quad E'(m) < 0 \ (m > m^*).$$

Combining the above:

1. $E(0^+) = E(\infty) = 0$.
2. $E(m) > 0$ on $(0, \infty)$.
3. $E'(m)$ changes sign exactly once from $+$ to $-$ at m^*.

Therefore $E(m)$ increases from 0 to a unique maximum $E(m^*)$ and then decreases back to 0, i.e. it is hump-shaped for all admissible parameter values λ, D, A.

K Others

The decomposition analysis shows that both the endogenous job destruction and the time-varying matching efficiency are critical for the Beveridge curve shifts. To understand their roles further, we analyze how the endogenous job separation comoves with the exogenous matching efficiencies. Figure K.15 is the scatter plots of the endogenous job separation rate (x-axis) and the matching efficiency (y-axis) for our baseline model (panel (a)) and the model without endogenous job destruction (panel (b)). The figure shows that the job destruction rate and matching efficiency significantly positively comove over the business cycle in our baseline model. The correlation is 0.982. This indicates that when the matching efficiency is higher, firms expect a greater chance of re-matching, leading to a higher job destruction rate. On the other hand, the job separation rate does not comove with the matching efficiency in the model with the exogenous separation (panel (b)) by construction.

To analyze the effect of this comovement on the Beveridge curve shift, we feed this comovement between the job separation rate and the matching efficiency exogenously

Figure K.15: Comovement between the job separation and the matching efficiency

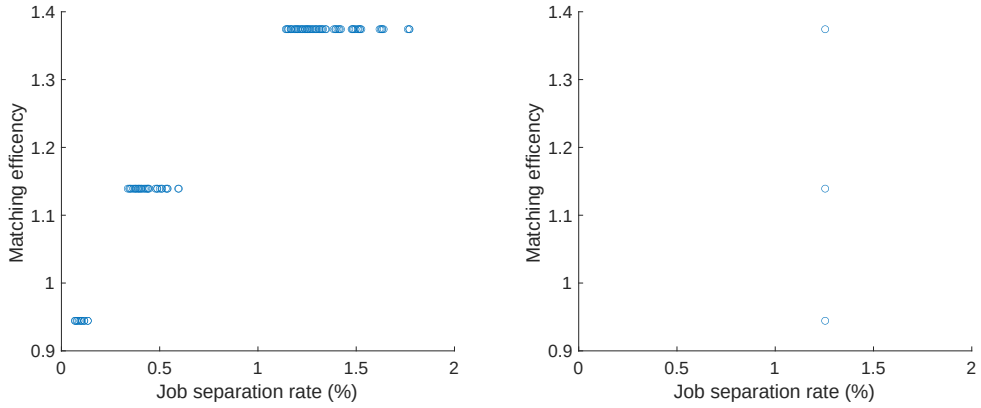

(a) Endogenous job destruction (b) Exogenous job destruction

to the exogenous job destruction model. Specifically, we first compute the expectation of the job separation rate conditional on each matching efficiency level and use this conditional expectation exogenously hard-wired to the matching efficiency fluctuations. Figure K.16 shows the Beveridge curve implied by the model with such exogenous co-movement. Now, the equilibrium displays shifts in the Beveridge curve similar to the baseline model despite the exogenous job destruction. This exercise shows that the comovement of job separation rate and the matching efficiency is the key channel for the shifts in the Beveridge curve.

Compared to the exogenous job destruction model (panel (b)), the baseline model's negative association displays greater convexity when the unemployment rate is lower. Table K.6 quantifies this greater convexity with a segmented regression showing the stronger non-linearity in the baseline model. That is, a marginal increase in the vacancy posting rate is likely to be associated with a smaller decline in the unemployment rate when the unemployment rate is lower. This nonlinearity in the baseline model is consistent with the observed pattern in the data. The comparison between the two Beveridge curves indicates that the empirically observed nonlinearity is captured in the equilibrium only when the model incorporates endogenous job destruction.

Table K.6: Spline fitting of the Beveridge curves

	VacancyRate	
	(1)	(2)
UnemploymentRate	-0.151^{***}	-0.142^{***}
	(0.004)	(0.009)
EndogenousBreak	0.038^{***}	
	(0.002)	
UnemploymentRate:EndogenousBreak	-1.185^{***}	
	(0.081)	
ExogenousBreak		0.015^{***}
		(0.001)
UnemploymentRate:ExogenousBreak		-0.158^{***}
		(0.011)
Constant	0.037^{***}	0.049^{***}
	(0.000)	(0.001)
Observations	15,500	15,500
R^2	0.140	0.240
Adjusted R^2	0.140	0.240
Residual Std. Error (df = 15496)	0.009	0.011
F Statistic (df = 3; 15496)	841.450^{***}	$1{,}631.049^{***}$

Notes: ***Significant at the 1 percent level.
**Significant at the 5 percent level.
*Significant at the 10 percent level.

Figure K.16: Beveridge curve from exogenous comovement between the job separation and the matching efficiency

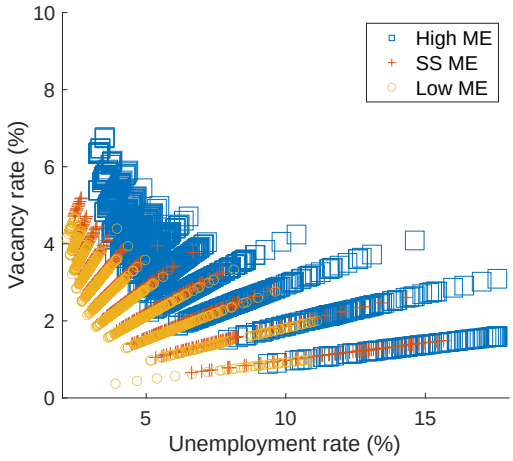

The segmented regressions for the Beveridge curve show that the Beveridge curve with endogenous separations has a stronger kink. Breaking points are chosen to maximiing the likelihood of the estimation and are at 3.25 % unemployment for endogenous job separations and 9.64 % for the Beveridge curve with exogenous job separations. The breaking point reflects the estimated steeper segment of the Beveridge curve and in this segment the coefficient on the unemployment rate are -1.34 and -0.30 respectively. For the flatter segments coefficients are similar at -0.151 and -0.142 respectively.

Figure K.17: Matching efficiency and the counter-cyclical unemployment benefit

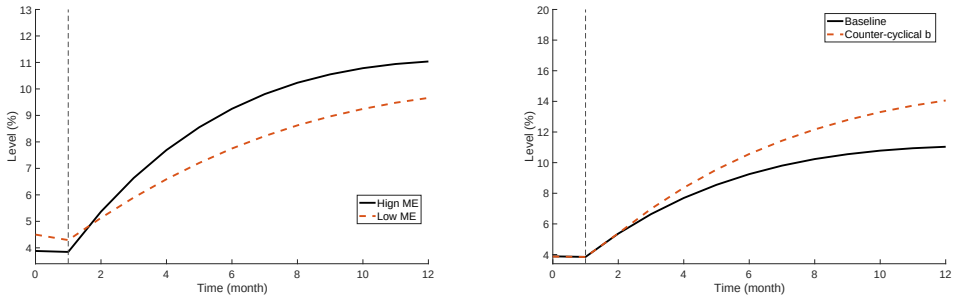

(a) ME-dependent shock responses (b) Counter-cyclical b during high ME

Panel (a) of Figure K.17 plots the unemployment response paths for Covid-19

recession (solid line) and the Great Recession (dashed line). The surrounding colored area indicates the 95% confidence interval. Despite the same exogenous state paths, the endogenous states display sharply distinct paths between the Covid-19 recession and the Great Recession. In particular, the high matching efficiency of the Covid-19, which is the key difference between the two conditioning states leads to a significantly greater response for around 10 months.

Panel (b) displays the global response paths for baseline (solid) and the baseline with the counter-cyclical unemployment benefit during the Covid-19 period. The counter-cyclical unemployment benefit significantly increases the responsiveness of the unemployment, which makes the unemployment rate 12 month after the initial shock reach around 14%, as observed in the data.

■

References

Abowd, John M and Arnold Zellner. 1985. "Estimating gross labor-force flows." *Journal of Business & Economic Statistics* 3 (3):254–283.

Ahn, Hie Joo and Leland D Crane. 2020. "Dynamic Beveridge curve accounting." *arXiv preprint arXiv:2003.00033* .

Elsby, Michael WL, Bart Hobijn, and Ayşegül Şahin. 2015. "On the importance of the participation margin for labor market fluctuations." *Journal of Monetary Economics* 72:64–82.

Hodrick, Robert J and Edward C Prescott. 1997. "Postwar US business cycles: an empirical investigation." *Journal of Money, credit, and Banking* :1–16.

Lee, Hanbaek. 2025. "Global Nonlinear Solutions in Sequence Space and the Generalized Transition Function." *Working paper* .

Pissarides, Christopher A. 2009. "The unemployment volatility puzzle: Is wage stickiness the answer?" *Econometrica* 77 (5):1339–1369.

Rotemberg, Julio J. 1999. "A heuristic method for extracting smooth trends from economic time series."

Sax, Christoph and Dirk Eddelbuettel. 2018. "Seasonal adjustment by x-13arima-seats in r." *Journal of Statistical Software* 87:1–17.